Journal of the Korean Society for Nondestructive Testing
Vol. 25, No. 3 (2005. 6)

Virtual Reality Presentation for Nondestructive Evaluation of Rebar Corrosion in Concrete based on Inverse BEM

Je-Woon Kyung*†, Masaru Yokota**, V. Leelalerkiet*** and Masayasu Ohtsu***

Abstract In order to evaluate the corrosion of reinforcing steel-bars (rebar) in concrete, a nondestructive evaluation by the half-cell potential method is currently applied. In this study, potentials measured on a concrete surface are compensated into those on the concrete-rebar interface by the inverse boundary element method (IBEM). Because these potentials are obtained three-dimensionally (3-D), 3-D visualization is desirable. To this end, a visualization system has been developed by using VRML (Virtual Reality Modeling Language). As an application, results of a reinforced concrete (RC) slab with corroded rebars are visualized and discussed.

Keywords : half-cell potential, nondestructive testing, inverse boundary element method, virtual reality modeling language, polarization resistance

Introduction

In recent decades, corrosion of rebars in reinforced concrete structures has become a major concern in concrete engineering (Emmons and Vaysburd, 1997). Due to salt attack, chloride ions penetrate through micro-pores inside concrete and reach to the surface of reinforcing steel-bars (rebar). Although the passive film on rebar can protect corrosion, the film would be destroyed by chloride ions. When concentration of chloride ions exceeds the threshold limit, corrosion is initiated. With supplying oxygen and water, electrochemical corrosion is initiated and accelerated. Expansion of corrosion products induces internal stress in concrete surrounding rebars and generates cracks which result in serious defects in reinforced concrete structures. Thus, nondestructive evaluation (NDE) for corrosion of rebars is to be performed prior to detection of visible cracks. So far, two nondestructive techniques of the half-cell potential and the polarization resistance are practically available. The former provides an indication of the probability of corrosion, while the latter is associated with information on the corrosion rate (Ohshiro et al., 1991).

For the half-cell potential measurement, the criterion to estimate the probability of corrosion has been already coded in ASTM C876 (ASTM C876, 1991). It is reported, however, that the potentials measured are too sensitive to moisture content, thickness of concrete cover, surface coating, resistivity of concrete and so forth (Misra and Uomoto, 1990). Consequently, estimation of corrosion by the half-cell potential is still inconclusive.

An essential drawback of the half-cell

Received: December 3, 2004, Accepted : May 11, 2005 * Research Institute of Technology, EJtech Co., Ltd, Seokjeong B/D, 204-5, Kumi-Dong Bundang-Gu, Gyeonggi-Do, Korea, ** Department of Civil Engineering, Shikoku Research Institute Inc. 2109 Yashima-Nishimachi, Takamastu 761-0192, Japan, *** Graduate School of Science and Technology, Kumamoto University 2-39-1 Kurokami, Kumamoto 860-8555, Japan, † Corresponding author: jwkyung@ejtech.net

potential measurement results from the fact that the potentials are measured not near rebars but on concrete surface. One compensation is to measure the potentials as close to rebars as probes of the electrode are embedded in concrete or are inserted into the bottom of bore holes (Tamura et al., 1992). Another compensation is to determine the potentials around rebars analytically. Although the boundary element method (BEM) was introduced (Otomaru et al., 1990), three-dimensional (3-D) analysis was not only time-consuming but also impractical.

In this paper, a simplified inversion by BEM (Kyung and Ohtsu, 2001) is applied to convert the potentials on concrete surface to those on rebars, taking into account the concrete resistivity. Although results of half-cell potential measurement are normally represented by two-dimensional contour mapping (Elsener, 2003), results are preferable to be visualized in three-dimensional (3-D) space. By employing VRML (Virtual Reality Modeling Language) technique, information of corrosion as well as locations of rebars can be visualized three-dimensionally.

A portable corrosion-meter (SRI-CM) is commercially available in Japan (Yokota, 1998), which can measure not only the half-cell potential, but also the polarization resistance and the concrete resistivity based on AC impedance technique. In VRML display, rebar arrangement is categorized as the type of rod arrangement. Based on results measured, corrosion degrees of rebars are classified. Thus, the development of VRML for visualizing the corrosion information is performed.

Theoretical Background

In the half-cell potential measurement, electric potential u in domain D (concrete) is measured at the surface. The potentials in concrete satisfies the following Laplace equation,

$$\nabla^2(u/R)=0 \text{ in D}, \tag{1}$$

where ∇ is the gradient operator and R is the concrete resistivity. In a homogeneous body, R is constant and then eqn. (1) becomes,

$$\nabla^2 u = 0 \text{ in D}, \tag{2}$$

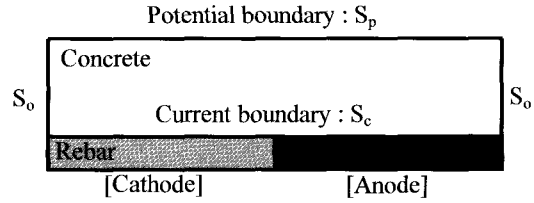

Fig. 1 Boundary conditions of reinforced concrete with macro-cell reaction.

As shown in Fig. 1, the boundary of concrete is classified into boundaries S_p, S_o and S_c. Concrete surface, where potentials are measured, corresponds to the potential boundary S_p. Another boundary S_o is electrically free where outward flow of the current is equal to zero.

The other is the current boundary Sc, which actually represents the interface between concrete and rebar. Under macro-cell corrosion, the interface with the rebar is classified into the anode region and the cathode region. These boundary conditions are given,

$$u = E(C.S.E) \quad \text{on Sp(potential boundary)}, \tag{3.a}$$

$$\frac{\partial}{\partial n}(u/R) = \begin{cases} 0 & \text{on So(electrically boundary)}, \\ f & \text{on So(current boundary)}, \end{cases} \tag{3.b, 3.c}$$

Here the potentials, E, are measured by utilizing a copper-copper sulfate half-cell electrode *(C.S.E)*, and n is the outward normal vector to the surface. f is the current flow at the interface boundary S_c.

Boundary Element Method and Inverse BEM

To solve eqn. (1) with the boundary conditions of eqn. (3), the boundary element method (BEM) is adopted. Provided that the concrete is referred to as homogeneous, solution $u(x)$ at point x can be solved by the boundary integral (Brebbia, 1978),

$$\frac{1}{2}u(x)=\int_S\left[G(x,y)\frac{\partial u}{\partial n}(y)-\frac{\partial G}{\partial n}(x,y)u(y)\right]dS \quad (4)$$

where S = S_p + S_o + S_c and points y are located on the boundary S surrounding the domain concrete D. $G(x,y)$ is the fundamental solution, as follows;

$$G(x,y)=\frac{1}{4\pi r} \text{ in the three-dimensional (3-D) body.} \quad (5)$$

Here r is the distance between x and y. The boundary is discretized into boundary meshes, prescribing potential u_j and current $\frac{\partial u_j}{\partial n}$ at point x_j on a boundary mesh. Digitizing eqn. (4), a set of linear algebraic equations are obtained,

$$\sum_{j=1}^{N}\left[\frac{\delta_{ij}}{2}+\frac{\partial G_{ij}}{\partial n}\right]\{u_j\}=\sum_{j=1}^{N}[G_{ij}]\left\{\frac{\partial u_j}{\partial n}\right\} \quad (i=1,\ N), \quad (6)$$

where N is the number of boundary meshes, δ_{ij} is Kronecker's delta and G_{ij} is the digitized fundamental solution between points x_i and x_j. Then, Internal potentials $u(x)$ are determined from the integral,

$$u(x)=\int_S\left[G(x,y)\frac{\partial u}{\partial n}(y)-\frac{\partial G}{\partial n}(x,y)u(y)\right]dS \quad (7)$$

Applying eqn. (7) to determine the potential at point x_i, which is actually located at the interface with rebar, the following equation is obtained as a digital form,

$$u_i=\sum_{j=1}^{M}\left[-\frac{\partial G_{ij}}{\partial n}R_j\right]u_j\Delta S \quad (8)$$

Here, the current boundary S_c is neglected, because $\partial u/\partial n(y)$ is always equal to zero.

The potential boundary S_p to be measured is divided into M rectangular elements of area $\triangle S$. As shown in Fig. 2, measuring point x_j at the center of the element is marked and potential u_j is measured at each location. Potentials, u_i, at the interface with rebars are computed as internal potentials, substituting potentials u_j and area $\triangle S$ into eqn. (8). R_j is the relative coefficient of concrete resistivity, which is obtained by taking into account inhomogeneity of concrete resistivities,

$$R_j = R_{ave}/R_{ej} \quad (9)$$

where R_{ave} is the averaged concrete resistivity of the measured surface and R_{ej} is the resistivity at each location. The procedure to apply eqn. (8) to determining compensated potentials is named as the inverse BEM (IBEM).

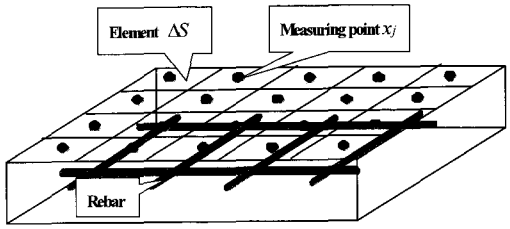

Fig. 2 Specimen and measured points.

Three-Dimensional Visualization by VRML

Visualization procedure is developed by using VRML (Virtual Reality Modeling Language). VRML is a real-time interactive program to simulate the virtual model in 3-D graphic. The geometry of concrete structure and the corrosion information on the rebar can be entirely displayed in 3-D space.

A result obtained at one measuring point by SRI-CM-II is listed in Table 1. Coordinates of locations, rebar diameter, rebar arrangement, cover thickness, polarized resistance, concrete resistance and half-cell potential are given. In the case that the geometrical information of rebar inside concrete is not available, radar is applicable to estimate locations, sizes and depths of rebars (Kyung and Ohtsu, 2001).

For 3-D graphic of VRML, rod arrangement of rebars is categorized as such arrangements as shown in Fig. 3. In the case of one rebar, the arrangement is defined as "1" for x-direction and "2" for y-direction, respectively. For rebars crossed, it is denoted as "3" when rebar in x-direction is over rebar in y-direction and "4" for vice versa.

In the half-cell potential measurement, the potentials are classified by the ASTM standard as given in Table 2. Based on the CEB criterion in Table 3 (CEB, 1997), the polarization resistances are also classified in three levels in Table 3.

Table 1 Listed results of measurement by SRI-CM-II

"Position No " " 1 "		"Title " " Specimen 101 B "	
"X Position (m) " 0.06 "		"Y Position (m) " 0.06 "	
"Rod Arrangement " "1"		"Rod Diameter d1 (cm) " 1.6 "	
"Rod Diameter d2 (cm) " 0.0		""Concrete Depth (cm) " 0.00	
"Guard Pole " " Guard on "		"Surface Area (cm^2)" 12.1	
"Input Voltage (mV) " 10.0		"Integral Times " 1"	
	" " Frequency1"	"Frequency2"	
"Frequency (mHz) "	10000.00	20.00	
"Absolute |Z| (Ohm) "	1977.6	5933.2	
"Phase difference "	-0.6	-33.8	
"Real Re|Z| (Ohm) "	1977.5	4930.4	
"Imaginary Im|Z| (Ohm)"	-20.7	-3300.6	
"Apparent Polarized Resistance (kOhm) " 12.620			
"Real Polarized Resistance (kOhm*cm^2) " 152.199			
"Corrosion Rate (microA/cm^2) " 0.1708			
"Concrete Resistivity (kOhm) " 1.977			
"Half-cell Potential (mV) " -55.2			

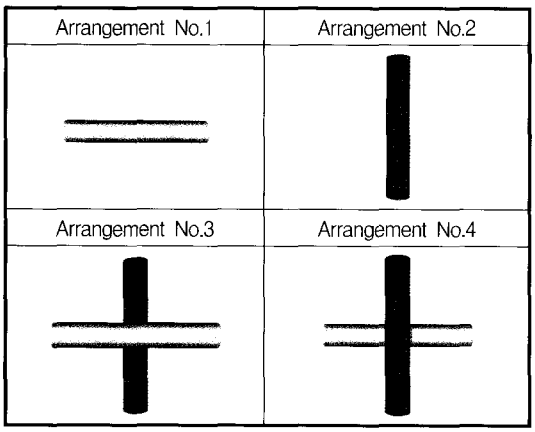

Fig. 3 Rod Arrangement

Table 2 ASTM criterion for half-cell potentials

Potential value (mV vs. CSE)	Criterion	Color of rebars	
- 200 < E	No corrosion	White	
- 350 < E ≦ 200	Uncertain	Orange	
E ≦ -350	Active corrosion	Red	

Table 3 CEB criterion for polarization resistances

Polarization resistance($k\Omega cm^2$)	Corrosion rate	Color of rebars	
$130 < R_P \leq 260$	Passive condition or very low	White	
$52 < R_P \leq 130$	Low to moderate	Orange	
$26 < R_P \leq 52$	Moderate to high		
$R_P \leq 26$	High	Red	

Experimental Results and Discussion

A reinforced concrete slab of dimensions 101 cm x 57 cm x 10 cm was tested. Rebars of 16 mm diameter were arranged at 15 mm cover-thickness. Configuration of the slab is shown in Fig. 4. To accelerate corrosion, 3% NaCl solution was mixed. Mixture proportion of concrete is given in Table 4. Compressive strength of concrete is 33.4 MPa, and the modulus of elasticity is 24 GPa at 28 days. The specimens were moisture-cured at 20℃ for 28 days. After removal from the mold, the top surface of the specimen and rebar surface out of it were epoxy-coated to protect from corrosion. The specimen was acceleratedly corroded by a cyclic wet-dry test for 14 weeks, being soaked in a reservoir for a week and dried for a week.

Table 4 Mixture proportion of concrete.

W/C (%)	s/a (%)	Weight of unit volume (kg/m^3)				NaCl (g)	AE (cc)	Slump (cm)	Air (%)
		W	C	S	G				
55	43.1	178	323	725	1145	329	129	9.1	6.5

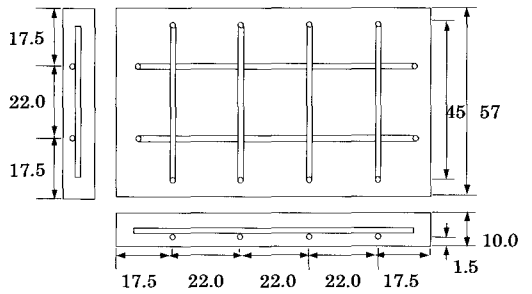

Fig. 4 Specimen and rebar arrangement (cm)

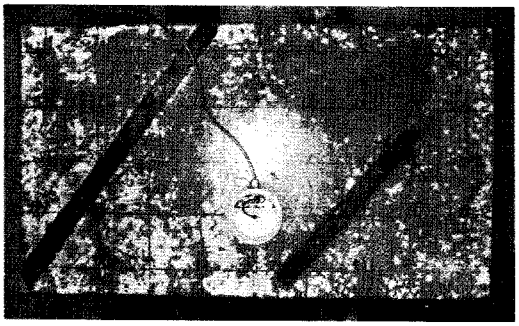

Fig. 5 SRI-CM measurement at the surface.

Table 5 Rod arrangements

Arrangement No.	Measurement number on the surface
0	1,3,5,7,9,19,21,23,25,27,37,39,41,43,45
1	10,12,14,16,18,28,30,32,34,36
2	2,4,6,8,20,22,24,26,38,40,42,44
3	Not existed
4	11,13,15,17,29,31,33,35

Half-cell potentials, concrete resistivities and polarization resistances at 45 points on the concrete surface were measured by SRI-CM as shown in Fig. 5. After the measurement, all data were transferred into a microcomputer and analyzed. The rod arrangements are summarized in Table 5. All results are three-dimensionally visualized by VRML in Fig. 6.

In Fig. 6(a), 3-D presentation of rebars and half-cell potentials measured on the surface are shown. The potentials are classified by ASTM standard in Table 2. It is found that the corrosi on at the right half is heavier than left half.

In Fig. 6(b), polarization resistances are plotted and classified based on the CEB criterion in Table 3. As for the polarization resistances, corrosion rates measured at the surface are not so high as corroded. By applying eqn. (8), the potentials at rebars were computed and then estimated from the ASTM criterion in Table 2. Results are given in Fig. 6(c), where the concrete resistivities were taken into account. After the measurements, the specimen was broken and rebars were removed to identify the corroded area. Results are shown in Fig. 6(d). It is found that rebar of the right-half portion is seriously corroded. White color indicates no visible rust on the surface. Orange shows a little rust at the

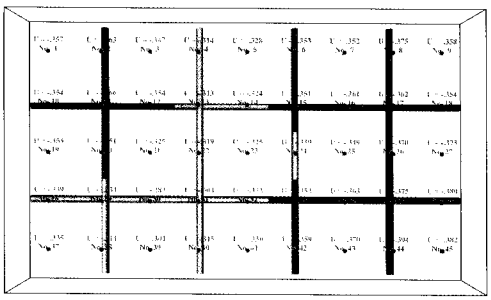

(a) Half-cell potential measurement (V, CSE).

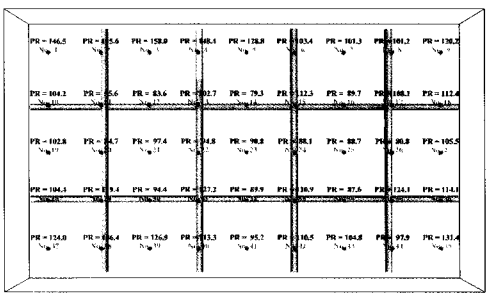

(b) Polarization resistance (kΩ.cm^2).

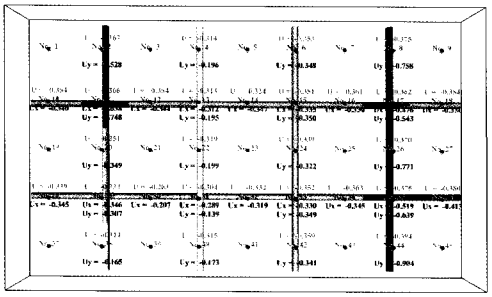

(c) Potentials on rebar by IBEM (V, CSE).

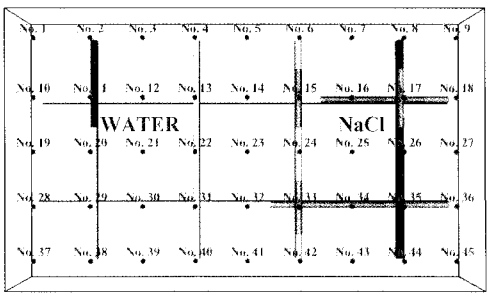

(d) Visual inspection.

Fig. 6 Results of measurement visualized by VRML.

on the surface. Orange shows a little rust at the surface. Red represents a heavy corrosion. Because corrosion rating is based on visible corrosion on the surface of the rebar, the pitting corrosion was not taken into account (Naish et al., 1990). As comparing results of visual inspection with the measurement, the best agreement is found in the results of IBEM. Thus, the measured potentials are effectively compensated by IBEM.

Conclusion

The geometry of concrete structure and the corrosion information on rebars can be visualized by VRML in three-dimensional space. Half-cell potentials are effectively compensated by IBEM (Inverse Boundary Element Method).

Consequently, three-dimensional visualization procedure for IBEM is developed. As a case study, a reinforced concrete slab was acceleratedly corroded and then measured. It is formed that the potentials compensated by IBEM could estimate the corroded region successfully, although conventional the half-cell potentials and the polarization resistances are in conclusive.

References

STM C876. (1991) *Standards test method for half-cell potentials of reinforcing steel in concrete*

Brebbia, CA. (1978) *The boundary element method for engineers,* London, Pentech Press

CEB (1997), Working Party V/4.1, *Strategies for Testing and Assessment of Concrete Structures Affected by Reinforcement Corrosion (draft.4),* BRI-CSTC-WTCB

Elsener, B. (2003) Half-cell potential measurements-Potential mapping on reinforced concrete structures, *Material and Construction,* Vol. 36, No. 261, pp. 461-471

Emmons, P.H. and Vaysburd, A.M. (1997) Corrosion protection in concrete repair: myth and reality, *Concrete International,* Vol. 19, pp. 47-56

Kyung, J.W. and Ohtsu, M. (2001) Improvement of half-cell potential measurement for nondestructive evaluation of rebar corrosion, *Proc. of JSCE,* Vol. 86, No. 2, pp. 828-829

Kyung, J.W. and Ohtsu, M. (2001) Study on half-cell potential measurement for NDE of rebar corrosion, *Structure and Faults and Repair,* London, UK, CD-ROM.

Misra, S. and Uomoto, T. (1990) Corrosion of rebars under different corrosions, *Proc. of JCI,* Vol. 12, No. 2, pp. 825-830

Nashi C., Harker, A., Carney, RFA. (1990) Concrete inspection: interpretation of potential and resistivity measurements. *Proc. of the Corrosion of Reinforcement in Concrete,* Elsevier Applied Science; pp. 314-332

Ohshiro, T., Tanikawa, S. and Goto, N. (1991) A study on corrosion evaluation of steel reinforcements in concrete, *Proc. of JCI,* Vol. 13, No. 1, pp. 503-508

Otomaru, M., Murakami, Y. and Ohtsu, M. (1990) Half-cell potentials analysis by BEM for corrosion monitoring, *Proc. of JCI,* Vol. 12, No. 1, pp. 539-544

Tamura, H., Nagayama, M. and Shimozawa, K. (1992) A case study on reinforcement corrosion in an existing RC structure, *Proc. of JCI,* Vol. 14, No. 1, pp. 763-768

Yokota, M. (1998) Study on corrosion monitoring of reinforcing steel bars in 36-year-old actual concrete structures, *Proc. of JSCE,* Vol. 20, No. 1, pp. 155-164